

UDC 541.6:547.13:546.47

ELECTRONIC STRUCTURE, CHARGE TRANSFER CHARACTER AND SPECTROSCOPIC PROPERTY OF ELECTROLUMINESCENT/PHOTOLUMINESCENT [ZnL₂] (HL = 2-(1H-BENZO[d]IMIDAZOL-2-YL)-4-BROMOPHENOL) STUDIED BY DENSITY FUNCTIONAL THEORY

Y.-P. Tong¹, Z. Jin¹, Y.-W. Lin²

¹*Department of Chemical Engineering, Huizhou University, Huizhou, P. R. China*
E-mail: typ2469@163.com

²*Department of Life Science, Huizhou University, Huizhou, P. R. China*

Received May, 17, 2014

In this paper the DFT-/TDDFT-based theoretical calculation results of the electroluminescence/photoluminescence zinc(II) chelate complex [ZnL₂] are presented, including the molecular geometry, electronic structure, charge transfer character of absorption and emission, effect of the Br group on the absorption/emission property and colors. The charge transfer character of UV-vis absorptions, and the nature of electroluminescence/photoluminescence are all due to the $\pi \rightarrow \pi^*$ ligand-to-ligand charge transfer transition (LLCT). The significant effect of the substituted Br group on the absorption/emission property and colors, and the Zn ligand bonding property of the main ionic interaction are analyzed and discussed in detail based on PDOS/OPDOS and the Mulliken population analyses. It is concluded that the introduction of substituted groups should significantly affect the electroluminescence/photoluminescence metal chelate complexes, with their absorption/emission property and colors being tuned.

DOI: 10.15372/JSC20150302

Keywords: Zn(II) chelate complex, 2-(1H-benzo[d]imidazol-2-yl)-4-bromophenol, theoretical calculation, electronic structure, LLCT, TDDFT, DOS/PDOS.

INTRODUCTION

The emitting transition metal complexes are currently of great research interest. Apart from the insight into fundamental excited state processes, there are numerous applications of such complexes, e.g. the new generation of displaying technology—organic light-emitting devices (OLEDs) [1–5], useful photochemical processes, energy and electron transfer, light-to-chemical energy conversion [6–8].

As far as zinc(II) complexes of N,O-donor phenol ligands are concerned, the number of compounds that emit efficiently in solid at room temperature has greatly increased over the past decade [9–11]. The uses of N,O-donor phenol ligands, such as 8-hydroxyquinoline [1, 12], 2-(2-hydroxyphenyl)benzimidazole [4], 2-(2-hydroxyphenyl)benzothiazole [4], and 2-(2-hydroxyphenyl)benzoxazole [4] have proved to be a successful strategy for strong OLED luminescent materials. The heterocycles with such ligands and the zinc(II) close-shell structure ensure that the ligand-centered states are properly located in energy, and therefore are responsible for the charge transfer of the relevant photophysical process. Some of these zinc-based molecular systems make use of the variations of heterocycles such as imidazole, thiazole, and oxazole, aimed at adjusting the cores of emitting complexes [4, 8].

Another strategy for modulating the emission of OLED emitting materials is to introduce a functional group to shift energy levels of molecular orbitals (MOs) relevant to the emission or to make an orbital level localized on the functional groups [13–15]. Based on this strategy, we calculated the 2-(1*H*-benzo[*d*]imidazol-2-yl)-4-bromophenol ligand with the bromo group as a substituent group. The functional bromo group might be an effective group for shifting the energy levels of MOs or taking part in the charge transfer of the relevant photophysical process. In this paper, we report the results of the density functional theory (DFT)-based calculation of the electronic structure, charge transfer character, and spectroscopic property of the zinc(II) complex, *i.e.* [ZnL₂] (HL = 2-(1*H*-benzo[*d*]imidazol-2-yl)-4-bromophenol).

COMPUTATIONAL DETAILS

DFT calculations were carried out using the Gaussian 98 program suite [16]. Becke's 3-parameter hybrid functional [17] with the LYP correlation functional [18, 19] (B3LYP) was used together with the Los Alamos effective core potential LanL2DZ [20–22]. As starting geometries, the molecular structures obtained at the semi-empirical AM1 level were used. [ZnL₂] was treated as a close-shell system using spin restricted DFT wavefunctions with the 6-31G** basis set for C, H, N, and O atoms, and the effective core potential basis set LanL2DZ for Zn and Br atoms. The converged wave functions were tested to confirm that they corresponded to the ground state surface. The second order derivative of the energy with respect to nuclear positions was evaluated to determine the nature of the stationary points, so that the vibrational frequencies calculated ascertained that the optimized structure was characterized to be stable (no imaginary frequencies). No symmetry constraints were applied and only the default convergence criteria were undertaken during optimization.

Based on the optimized geometries, TDDFT calculations were performed at the same B3LYP level, and with the same basis sets as in the DFT calculations for C, H, N, O, Br, and Zn atoms to calculate the vertical electron transition energies. The electron density diagrams of MOs were obtained with the Molden 3.5 graphics program [23].

Following the DFT and TDDFT calculations, the density of states (DOS) and/or the partial density of states (PDOS) and the overlap population density of states (OPDOS) diagrams were usually employed for the further electronic structure analysis. The DOS and/or the PDOS and OPDOS diagrams arise from the Mulliken population analysis (MPA)-based molecular orbital calculations, and can give a more realistic picture of the electronic structure of molecules. Important bond properties between Zn(II) centers and ligand donor atoms were obtained by a further charge decomposition analysis, MO analysis in terms of molecular fragment orbital contributions and molecular fragment orbital interactions. The DOS and/or PDOS and OPDOS spectra were created by convoluting the MO information with Gaussian curves of full width at half maximum (fwhm) = 0.3 eV [24].

RESULTS AND DISCUSSION

Structure. The structure of [ZnL₂] was optimized at the B3LYP/6-31G**/LanL2DZ level of theory (Fig. 1). The calculated geometrical parameters are shown in Table 1. Although the adopted basis set is not relatively high accurate, the current theoretical level gives reasonable results, being comparable to the experimental ones of similar complexes [25].

The complex shows a pseudo-tetrahedral arrangement of ligands (Fig. 1) around the metal Zn(II) atom with bond angles around Zn(II) of

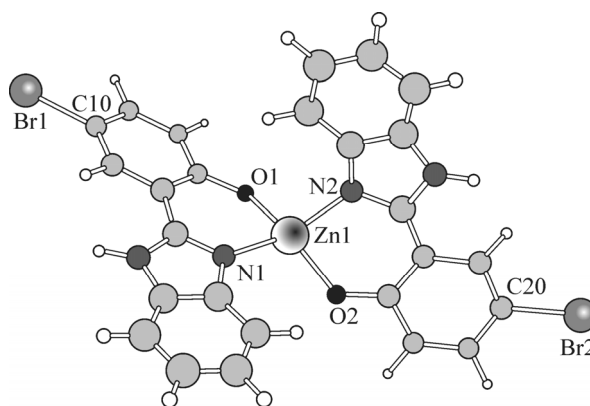


Fig. 1. View of the calculated geometrical structure of [ZnL₂]

Table 1

Selected calculated bond lengths and angles (Å, deg.) of [ZnL₂]

Zn1—O1	1.954
Zn1—O2	1.949
C10—Br1	1.974
Zn1—N1	2.073
Zn1—N2	2.078
C20—Br2	1.973
O1—Zn1—N1	91.7
O1—Zn1—O2	129.0
O2—Zn1—N2	91.7
O1—Zn1—N2	114.6
O2—Zn1—N1	112.6
N1—Zn1—N2	120.2

Table 2

Percentage fragment compositions of the frontier Kohn—Sham orbitals of [ZnL₂]

Orbitals	Energy, eV	Zn, %	L ⁻ , %	
			BIP, %	Br, %
LUMO+5	-0.14	0	58	42
LUMO+4	-0.14	0	57	43
LUMO+3	-0.19	1	96	2
LUMO+2	-0.21	2	97	1
LUMO+1	-1.55	0	100	0
LUMO	-1.58	0	100	0
HOMO	-5.44	1	91	8
HOMO-1	-5.46	1	91	8
HOMO-2	-6.46	0	97	3
HOMO-3	-6.47	0	97	3
HOMO-4	-6.72	0	100	0
HOMO-5	-6.75	0	100	0

91.7—129.0°. The L⁻ ligands are almost coplanar. As expected, the Zn—N bond distances are longer than the Zn—O distances, reflecting the fact that the Zn—N bond is weaker than the Zn—O bond.

Electronic structure. [ZnL₂] was studied systematically at the DFT-/TDDFT-based B3LYP/6-31G**/LanL2DZ level aimed at understanding its geometrical and electronic structure, spectroscopic properties, and charge transfer properties. The orbital energy level scheme may provide meaningful information on the orbital structure, and the coupling of the various one-electron states involved in the optical excitations.

Fig. 2 shows the diagram of the calculated energy levels of the frontier orbitals. Two-electron population method was applied in this paper to treat electron overlap populations between different molecular fragments. Six highest occupied molecular orbitals (HOMOs) are mainly composed of the L⁻ ligand. All these orbitals have the π -symmetry. The contribution of the Zn(II) center orbitals to these MOs does not exceed 1 % (Table 2). Similarly, the six lowest unoccupied MOs are mainly composed of the L⁻ ligand, and the contribution of the Zn(II) center orbitals to these MOs does not exceed 2 % (Table 2). Among six orbitals, LUMO to LUMO+3 orbitals have the π^* -symmetry, while LUMO+4 and LUMO+5 orbitals have the σ^* -symmetry of the C—Br bond.

[ZnL₂] consists of a Zn(II) center and two L⁻ ligands. As shown in Fig. 2, the frontier orbitals are obviously distributed in "doublets" in energy and these orbital "doublets" are mainly composed of the contributions of two L⁻ ligands (L⁻ containing the Br subgroup and the 2-(1H-benzoimidazol-2-yl)-phenolate subgroup denoted as BIP) with negligible contributions from the Zn(II) center (Table 2, Fig. 2). These orbital "doublets" are HOMO/HOMO-1, HOMO-2/HOMO-3, HOMO-4/HOMO-5, LUMO/LUMO+1, LUMO+2/LUMO+3, LUMO+4/LUMO+5, etc., in which the "doublets" (LUMO/LUMO+1) are the poorest in degeneration. These almost degenerate "doublet" orbitals can be taken into account by the point group theory since [ZnL₂] is not a perfect C_{2v} group, but an approximate C_{2v} group molecule. The symmetry loss must lead to the energy split of the degenerate orbitals, thus, the orbital "doublets" can be expected.

The wavelengths and colors of electroluminescence/photoluminescence relevant metal chelate complexes can be modulated *via* the introduction of substituted groups, since these groups may contribute to the frontier orbitals. As shown in Table 2, the HOMO/HOMO-1 "doublet" orbitals have a greater contribution from the substituted Br group (8 %) than other "doublet" orbitals, suggesting that the Br group will significantly stabilize the HOMO/HOMO-1 "doublet" orbitals, and further affects

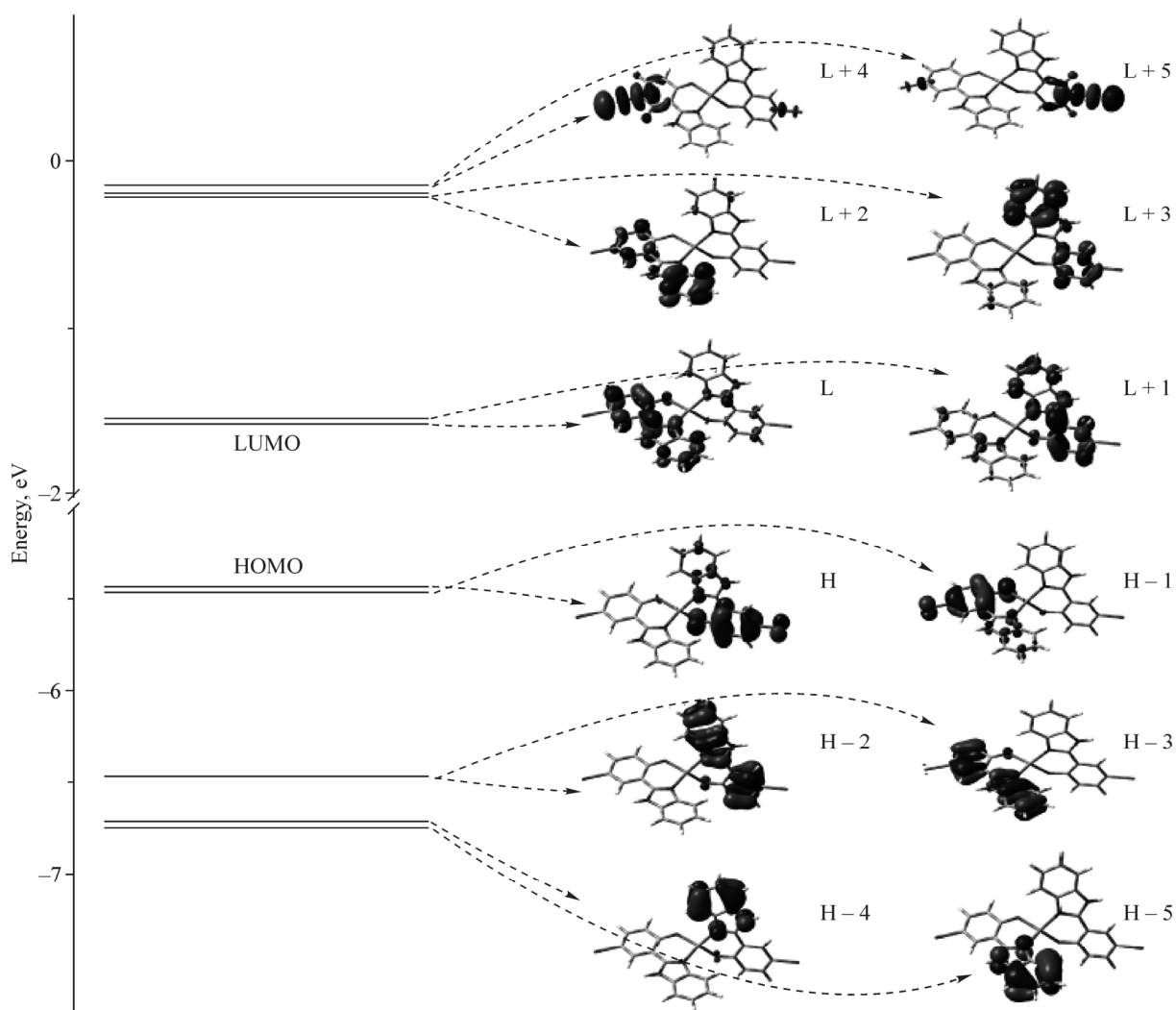


Fig. 2. Energy levels and shapes of the relevant frontier orbitals of $[\text{ZnL}_2]$. The L^- ligand orbitals are distributed in "doublets" in energy, and the Zn(II) orbitals are absent from the frontier orbitals

the HOMO—LUMO energy gap. Thus, the wavelength or color of optical absorption or emission may be tuned.

In theory, the strong optical absorptions correspond to transitions with large transition matrix elements. The dipole transition from HOMO to LUMO has very small matrix elements, and HOMO-3 to LUMO, HOMO-2 to LUMO+1, HOMO to LUMO+1, and HOMO-1 to LUMO, *etc.* have relatively larger matrix elements based on the electron density diagrams of orbitals (Fig. 2), because the spatial overlap between the transition orbitals is quite less for the former, while those are relatively larger for the latter.

In addition, the occupied L^- ligand orbitals with the π symmetry are only strongly coupled to their unoccupied orbitals with the π^* symmetry. Therefore, the strongest absorbance does correspond to transitions from the occupied L^- ligand orbitals with the π symmetry to the unoccupied L^- ligand orbitals with the π^* symmetry. Thus, both Zn center and LUMO+4/LUMO+5 orbitals with the σ^* symmetry should not be involved in the optical transitions. The above theoretical presumptions need confirmation from more advanced calculations of the excitation energies at the TDDFT level.

Excited state and charge transfer character of electronic transitions. In general, the features of the electronic spectra of transition metal complexes can be interpreted as $d-d$, metal-to-ligand

charge transfer (MLCT), ligand-to-metal charge transfer (LMCT), ligand-to-ligand charge transfer (LLCT), or intra-ligand charge transfer (ILCT) transitions. However, such descriptions are only appropriate in the weak metal-ligand coupling limit, where "pure" CT excited states are most rigorously defined. When the metal-ligand coupling is high, the MOs are of a mixed metal-ligand character, and the descriptions of electron transitions such as pure $d-d$, MLCT, LMCT, LLCT, or ILCT become approximate [26].

As partial CT transitions, the following definition of the CT character can be used:

$$CT_I(\%) = 100(P_g(M) - P_I(M)),$$

where $P_g(M)$ and $P_I(M)$ are the electron densities on metal in the ground and excited electronic states respectively. Positive CT_I values correspond to MLCT transitions; negative CT_I values correspond to LMCT transitions.

This definition can be rewritten using the atomic orbital (AO) contributions to MOs. Then, the CT character for the HOMO $-x$ \rightarrow LUMO $+y$ excitation is [26]

$$CT(\%) = \%(\text{M})_{\text{HOMO}-x} - \%(\text{M})_{\text{LUMO}+y}.$$

If the excited state is formed by more than one single-electron excitation, then the CT character of this excited state is expressed as a sum of CT characters of each participating excitation $\varphi_i \rightarrow \varphi_a$

$$CT_I(\%) = \sum_{i,a} [C_I(i-a)]^2 (\%(\text{M})_i - \%(\text{M})_a),$$

where $C_I(i \rightarrow a)$ are the corresponding coefficients of the I -th eigenvector of the CIS matrix. So, one can use the AO contributions to MOs to probe the nature of the electronic transitions.

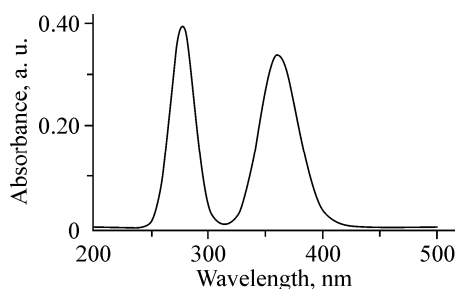
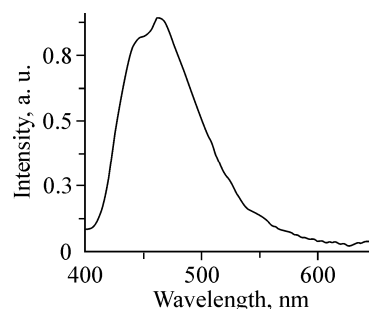
Table 3 shows the TDDFT-based results of the calculated Uv-vis absorption peaks, oscillator strengths, transition configurations, transition properties, and CT values.

The simulated UV-Vis spectrum is shown in Fig. 3. The strongest absorption peak is located at *ca.* 278.1 nm with the oscillator strength f of 0.2874 (Table 3). It is related to the principal electronic transition $S_0 \rightarrow S_8$. The transitions are assigned to LLCT transitions in nature from the π (L^-) orbitals (HOMO-2/HOMO-3 "doublets") to π^* (L^-) orbitals (LUMO). The weak charge transfer from the Br fragment to the BIP fragment is also observed (3%), while the central Zn(II) atom is not involved in the charge transfer process. The other calculated strong absorption peaks located at 358.9 nm (f 0.1994), 361.7 nm (f 0.1818), 279.3 nm (f 0.1414), 357.3 nm (f 0.1322), and 277.0 nm (f 0.1266) are related to the principal electronic transitions $S_0 \rightarrow S_3$, $S_0 \rightarrow S_2$, $S_0 \rightarrow S_7$, $S_0 \rightarrow S_4$, and $S_0 \rightarrow S_9$

Table 3

Calculated Uv-vis absorption bands, oscillator strengths, transition configurations, and transition properties of [ZnL₂]

	Calcd. λ , nm	Oscillator strength	Transition configuration	Zn, %	$L^-, \%$	
					BIP, %	Br, %
1	364.1	0.0485	HOMO \rightarrow LUMO (94 %)	1 \rightarrow 0 (-1)	91 \rightarrow 100 (9)	8 \rightarrow 0 (-8)
2	361.7	0.1818	HOMO-1 \rightarrow LUMO (56 %) HOMO \rightarrow LUMO+1 (30 %)	1 \rightarrow 0 (-1)	91 \rightarrow 100 (9)	8 \rightarrow 0 (-8)
3	358.9	0.1994	HOMO \rightarrow LUMO+1 (55 %) HOMO-1 \rightarrow LUMO (-28 %)	1 \rightarrow 0 (-1)	91 \rightarrow 100 (9)	8 \rightarrow 0 (-8)
4	357.3	0.1322	HOMO-1 \rightarrow LUMO+1 (90 %)	1 \rightarrow 0 (-1)	91 \rightarrow 100 (9)	8 \rightarrow 0 (-8)
7	279.3	0.1444	HOMO-3 \rightarrow LUMO (34 %) HOMO-2 \rightarrow LUMO (38 %)	0 \rightarrow 0 (0)	97 \rightarrow 100 (3)	3 \rightarrow 0 (-3)
8	278.1	0.2874	HOMO-3 \rightarrow LUMO (45 %) HOMO-2 \rightarrow LUMO (-35 %)	0 \rightarrow 0 (0)	97 \rightarrow 100 (3)	3 \rightarrow 0 (-3)
9	277.0	0.1266	HOMO-2 \rightarrow LUMO+1 (65 %) HOMO-2 \rightarrow LUMO (-22 %)	0 \rightarrow 0 (0)	97 \rightarrow 100 (3)	3 \rightarrow 0 (-3)

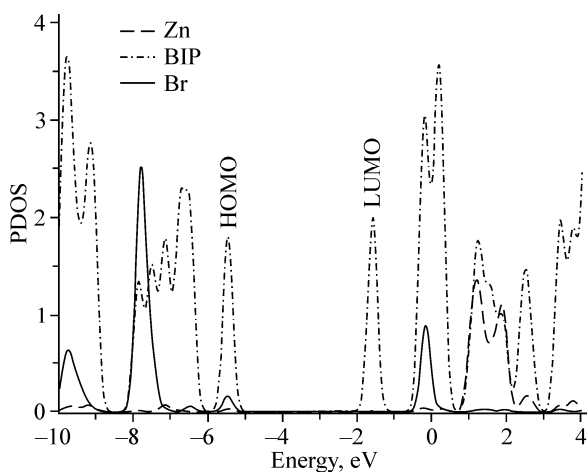
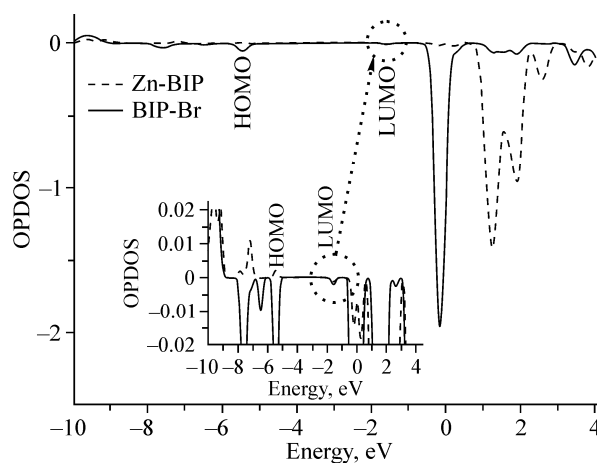
Fig. 3. UV-Vis absorption spectrum of $[ZnL_2]$ Fig. 4. Emission spectrum of $[ZnL_2]$

respectively. The respective transitions are all assigned to LLCT transitions in nature from the π (L^-) "doublet" orbitals to the π^* (L^-) "doublet" orbitals. The weak-to-moderate charge transfer from the Br fragment to the BIP fragment is also observed (3–8 %), while the central Zn(II) atom is not involved in the charge transfer process. No σ^* (L^-) "doublet" orbitals (LUMO+4/LUMO+5) are observed in the calculated optical transitions, in agreement with the above presumptions.

According to the TDDFT calculation, the lowest energy $S_0 \rightarrow S_1$ transition (364.1 nm, f 0.0485), corresponds to the LLCT transition π (L^-) orbital (HOMO) \rightarrow π^* (L^-) orbital (LUMO) (Table 3). However, the calculated intensity of this transition is too low to be observed experimentally owing to the small f value. The moderate charge transfer from the Br fragment to the BIP fragment is observed (8 %), while the central Zn(II) atom is not involved in the charge transfer process. The weak feature of this peak is in agreement with the presumption that the HOMO \rightarrow LUMO transition has a very small matrix element. Although it is weak in light absorption and LLCT in nature, according to the energy gap law for radiationless deactivation [28–32], the nature of the important electronic origin of the photoluminescent transition of $[ZnL_2]$ should be LLCT. It emits bluish-green light in the solid state with the maximum peak at *ca.* 464 nm (Fig. 4).

According to the above discussions, it is concluded that the Br group plays a significant role in the important optical transitions (electronic absorption and emission) for electroluminescence/photoluminescence relevant metal chelate complex $[ZnL_2]$. The electronic absorptions are LLCT in nature, and the electroluminescent/photoluminescent property is also LLCT.

Bonding property of metal-ligand interactions. DOS or PDOS, and OPDOS analysis helps to determine the electronic structure and understand the detailed bonding between different fragments of a molecular system. The PDOS and OPDOS are plotted in Figs. 5 and 6, respectively. The analysis

Fig. 5. PDOS diagram of $[ZnL_2]$ Fig. 6. OPDOS diagram of $[ZnL_2]$. The inset shows that the LUMO area has a very small negative OPDOS value

revealed that the mixing between the Zn(II) center and the L^- ligand is much less, and the mixing between the BIP and Br fragments is much larger in the energy region of -10.0 — -5.0 eV. Non-bonding interactions between Zn(II) and the L^- ligand are observed just near the HOMO level, and in vicinity of the LUMO level (a very small negative OPDOS value, inset in Fig. 6). The Zn-ligand interaction is almost non-bonding in the energy region of -10.0 — -6.0 eV, as OPDOS values are almost zero, while the BIP-Br interaction within the L^- ligand is anti-bonding near HOMO and non-bonding near LUMO, as the OPDOS values are negative for the former and zero for the latter. Due to the fact that the Zn— L^- ligand interaction below the HOMO level in energy are all basically weak bonding or non-bonding in nature and are filled, it is suggested that the Zn— L^- ligand interaction is weak. However, the BIP-Br interaction within the L^- ligand below the HOMO level in energy is more complicated, since it is anti-bonding and bonding in nature.

The Mulliken population analysis shows that the net charge of the Zn(II) center is a 1.08 positive charge. The electron transfer is mainly into the $4s$ orbital of the Zn atom. The PDOS and OPDOS diagrams suggest a relatively small degree of covalency of the Zn-BIP bond (Figs. 5 and 6). This is in approximate agreement with the electronic population on the Zn atom. It is reasonable to propose the qualitative bonding picture which includes mainly the ionic interaction between the central Zn atom and the L^- ligand.

CONCLUSIONS

In this paper, theoretical calculations of the electroluminescence/photoluminescence zinc(II) complex $[ZnL_2]$ (HL = 2-(1*H*-benzo[*d*]imidazol-2-yl)-4-bromophenol) were performed at the DFT and TDDFT level. The calculated results of the molecular geometry, electronic structure, charge transfer character of absorption and emission, the Br group effect on the absorption/emission property and colors have been presented in detail. The simulated Uv-vis spectrum and the charge transfer character related to Uv-vis absorptions ($\pi \rightarrow \pi^*$ LLCT) are given. The electroluminescence/photoluminescence is also $\pi \rightarrow \pi^*$ LLCT in nature. Based on PDOS/OPDOS and Mulliken population analyses, the Zn ligand bonding property is mainly the ionic interaction. Because of the fact that the substituted Br group exerts a significant effect on the absorption/emission property and colors, it is concluded that the introduction of different substituted groups should significantly affect the electroluminescence/photoluminescence relevant metal chelate complexes, with their absorption/emission property and colors being tuned.

This work was supported by the Natural Science Foundation of Guangdong Province, China (No. S2012010010311); the National Natural Science Foundation of China (No. 21271080); the General science and technology project on integration of production, education and research, Guangdong Province, China (No. 2012B091100200); the Scientific Foundation of Educational Commission of Guangdong Province, China (No. 2012KJ CX0098).

REFERENCES

1. Tang C.W., VanSlyke S.A. // *Appl. Phys. Lett.* – 1987. – **51**. – P. 913.
2. Cui Y., Liu Q.-D., Bai D.-R., Jia W.-L., Tao Y., Wang S. // *Inorg. Chem.* – 2005. – **44**. – P. 601.
3. Wang S. // *Coord. Chem. Rev.* – 2001. – **215**. – P. 79.
4. Tong Y.-P., Zheng S.-L., Chen X.-M. // *Inorg. Chem.* – 2005. – **44**. – P. 4270.
5. Yu G., Yin S., Liu Y., Shuai Z., Zhu D. // *J. Amer. Chem. Soc.* – 2003. – **125**. – P. 14816.
6. Connick W.B., Mskowski V.M., Houlding V.H., Gray H.B. // *Inorg. Chem.* – 2000. – **39**. – P. 2585.
7. Khairutdinov R., Hurst J.K. // *Nature*. – 1999. – **402**. – P. 509.
8. Kim T.S., Okubo T., Mitani T. // *Chem. Mater.* – 2003. – **15**. – P. 4949.
9. Kai Y., Moraita M., Yasuka N., Kasai N. // *Bull. Chem. Soc. Jpn.* – 1985. – **58**. – P. 1631.
10. Yu G., Liu Y., Song Y., Wu X., Zhu D. // *Synth. Met.* – 2001. – **117**. – P. 211.
11. Wang P., Hong Z., Xie Z., Tong S., Wong O., Lee C.-S., Wong N., Hung L., Lee S. // *Chem. Commun.* – 2003. – P. 1664.
12. Sapochak L.S., Benincasa F.E., Schofield R.S., Baker J.L., Riccio K.K.C., Fogarty D., Kohlmann H., Ferris K.F., Burrows P.E. // *J. Amer. Chem. Soc.* – 2002. – **124**. – P. 6119.

13. Sugimoto M., Anzai M., Sakanoue K., Sakaki S. // *Appl. Phys. Lett.* – 2001. – **79**. – P. 2348.
14. Chen C.H., Shi J. // *Coord. Chem. Rev.* – 1998. – **171**. – P. 161.
15. Kido J., Iizumi Y. // *Chem. Lett.* – 1997. – P. 963.
16. Frisch M.J., Trucks G.W., Schlegel H.B., Scuseria G.E., Robb M.A., Cheeseman J.R., Zakrzewski V.G., Montgomery J.A., Stratmann R.E., Burant J.C., Dapprich S., Millam J.M., Daniels A.D., Kudin K.N., Strain M.C., Farkas O., Tomasi J., Barone V., Cossi M., Cammi R., Mennucci B., Pomelli C., Adamo C., Clifford S., Ochterski J., Petersson G.A., Ayala P.Y., Cui Q., Morokuma K., Malick D.K., Rabuck A.D., Raghavachari K., Foresman J.B., Cioslowski J., Ortiz J.V., Stefanov B.B., Liu G., Liashenko A., Piskorz P., Komaromi I., Gomperts R., Martin R.L., Fox D.J., Keith T., Al-Laham M.A., Peng C.Y., Nanayakkara A., Gonzalez C., Challacombe M., Gill P.M.W., Johnson B.G., Chen W., Wong M.W., Andres J.L., Head-Gordon M., Replogle E.S., Pople J.A. GAUSSIAN 03, Revision C.02, Gaussian Inc., Pittsburgh, PA, 2003.
17. Becke A.D. // *J. Chem. Phys.* – 1993. – **98**. – P. 5648.
18. Lee C., Yang W., Parr R.G. // *Phys. Rev. B.* – 1988. – **B37**. – P. 785.
19. McLean A.D., Chandler G.S. // *J. Chem. Phys.* – 1980. – **72**. – P. 5639.
20. Hay P.J., Wadt W.R. // *J. Chem. Phys.* – 1985. – **82**. – P. 270.
21. Hay P.J., Wadt W.R. // *J. Chem. Phys.* – 1985. – **82**. – P. 284.
22. Hay P.J., Wadt W.R. // *J. Chem. Phys.* – 1985. – **82**. – P. 299.
23. Schaftenaar G. Molden, Version 35, CAOS/CAMM Center, Nijmegen, Toernooiveld, 1999.
24. O'Boyle N.M., Tenderholt A.L., Langner K.M. // *J. Comp. Chem.* – 2008. – **29**. – P. 839.
25. Lin Y.-W., Tong Y.-P. // *Inorg. Chem. Commun.* – 2009. – **12**. – P. 208.
26. Gorelsky S.I., Lever A.B.P. // *Canad. J. Anal. Sci. Spectrosc.* – 2003. – **48**. – P. 1.
27. Turro N.J. *Modern Molecular Photochemistry.* – Sausalito: University Science Books, CA, 1991.
28. Klessinger J.M., Michl J. *Excited States, Photochemistry of Organic Molecules.* – New York: VCH, 1995, references cited therein.
29. Scaltrito D.V., Thompson D.W., O'Callaghan J.A., Meyer G.J. // *Coord. Chem. Rev.* – 2000. – **208**. – P. 243, references cited therein.
30. Tong Y.-P., Zheng S.-L., Chen X.-M. // *J. Mol. Struct.* – 2007. – **826**. – P. 104.
31. Tong Y.-P., Zheng S.-L., Chen X.-M. // *Aust. J. Chem.* – 2006. – **59**. – P. 653.
32. Tong Y.-P., Lin Y.-W. // *Synth. Met.* – 2010. – **160**. – P. 1662.